A Magnetometer-based Method for In-situ Syncing of Wearable Inertial Measurement Units

Thomas J Gilbert [1,*], Zexiao Lin [1], Sally Day [1], Antonia F de C Hamilton [2] and Jamie A Ward [3]

[1] *Engineering Department, University College London, United Kingdom*
[2] *Institute of Cognitive Neuroscience, University College London, United Kingdom*
[3] *Department of Computer Science, Goldsmiths, University of London, United Kingdom*

Correspondence*:
Thomas J Gilbert
thomas.j.gilbert@ucl.ac.uk

Jamie A Ward
jamie@jamieward.net

ABSTRACT

This paper presents a novel method to synchronise multiple wireless inertial measurement unit sensors (IMU) using their onboard magnetometers. The basic method uses an external electromagnetic pulse to create a known event measured by the magnetometer of multiple IMUs and in turn uses this to synchronise the devices. An initial evaluation using 4 commercial IMUs reveals a maximum error of 40ms per hour as limited by a 25 Hz sample rate. Building on this we introduce a novel method to improve synchronisation beyond the limitations imposed by the sample rate and evaluate this in a further study using 8 IMUs. We show that a sequence of electromagnetic pulses, in total lasting less than 3-seconds, can reduce the maximum synchronisation error to 8ms (for 25 Hz sample rate, and accounting for the transient response time of the magnetic field generator). An advantage of this method is that it can be applied to several devices, either simultaneously or individually, without the need to remove them from the context in which they are being used. This makes the approach particularly suited to synchronising multi-person on-body sensors while they are being worn.

1 INTRODUCTION

In the last decade there has been a huge growth in applications for IMU-enabled wearable and IOT devices. Applications stretch from the wider topics of human activity recognition Bian et al. (2022); Bulling et al. (2014) and multi-sensor fusion Gravina et al. (2017), to studies measuring social interaction and engagement in real-world settings, e.g. Sun et al. (2023); Gao et al. (2020). Many such applications require precise synchronisation between separate IMU devices, an issue that is made all the more difficult over longer timescales. For example in Ward et al. (2018), recordings of multiple autistic children and actors performing together over several hours are analysed to uncover fine-grained moments of motion synchrony. Similarly, Gao et al. (2020) records detailed physical and physiological data from students in class over a period of several weeks. In both of these examples, data is recorded offline on individual devices and then uploaded at the end of a session. To perform any time-series analysis or fine-grained fusion of such data, then precise synchronisation between data sources is essential.

Most commercial IMUs include an on-board real-time clock (RTC). Unfortunately, typical RTCs tend to drift over time, such that over a long recording duration the clocks across multiple devices will vary wildly. This means that RTC-only based synchronisation is not a viable option for longer experiments.

Efforts to overcome the synchronisation problem can be grouped into three categories: network-based, event/gesture-based, or a combination. Much work has been done using Network Time Protocol (NTP) Raman et al. (2020); Wang et al. (2019); Li and Sinha (2012); Yan et al. (2019) and Precision Time Protocol (PTP) Idrees et al. (2020) for time synchrony in IoT, however such protocols have been proven to be noisy with errors exceeding 1800ms or impractical for common mobile sensing task Luo et al. (2017). Moreover, most commercial IMU devices do not have network options requiring external network chips to be included. One solution is to use sync events within the data itself, creating a common signal across different sensors and sensor types to facilitate temporal alignment. Kinetic events are most commonly used requiring the experimenter or participant to make a predefined movement, such as clapping or hitting the table Wang et al. (2019); Ward et al. (2017); Plotz et al. (2012), or even tapping the ear Hoelzemann et al. (2019). Bannach et al. (2009) show that synchronising events can be collected from various sensors, including sound and light sensors. LED-sourced light has been used previously to update clock signals in IoT devices Guo et al. (2016). ECG sensors have also been used to synchronise across wearable devices Wolling et al. (2021a) Wolling et al. (2021b).

Electromagnetic fields have been previously used to synchronise wireless sensor networks (WSN). Rowe et al. (2009) developed an LC tank receiver circuit tuned to 60 Hz such that they can use the stochastic nature of the magnetic fields radiating from AC power lines to create a synchronising signal. The method described achieves an average synchronisation error of less than 1 ms. This requires the WSN to be near AC power lines which might limit the use in wearable applications (e.g. when outdoors). Another limitation pointed out by Rowe et al. (2009) is that the system temporarily fails when any objects get within proximity of the LC circuit creating a very strict synchronising environment. Additionally, this method requires adding new hardware to commercial IMU devices.

In a recent work most similar to that presented here, Spilz and Munz (2023) demonstrate the use of inductors to create an electromagnetic event which is captured by magnetometers on Shimmer3 IMUs. They are able to achieve sub-sample period accuracy by looking at which transient responses have a sample present. This technique allows them to achieve a 2.6ms offset error using 100Hz magnetometers, requiring a synchronisation time of 8 seconds. The method described is highly dependent on the IMUs being still relative to the inductors, therefore a synchronisation box was developed to hold the IMUs in place. As the method described relies on a sample ”hitting” a transient response, the chances of this happening decrease as the sample rate decreases, increasing the synchronisation time proportionately to the decrease in sample frequency. Another limitation of the method is that all the IMUs must be synchronised at the same time meaning experiments are limited to the number of inductors in the synchronisation box.

Most of the previous methods, particularly those requiring a kinetic event, can be disruptive often requiring the subjects to stop what they are doing to perform an action or even in some cases transfer their wearable sensors to holders. The method proposed by this paper minimizes these disruptions and replaces them with a wireless solution that requires no new hardware to be added to the commercial IMU devices.

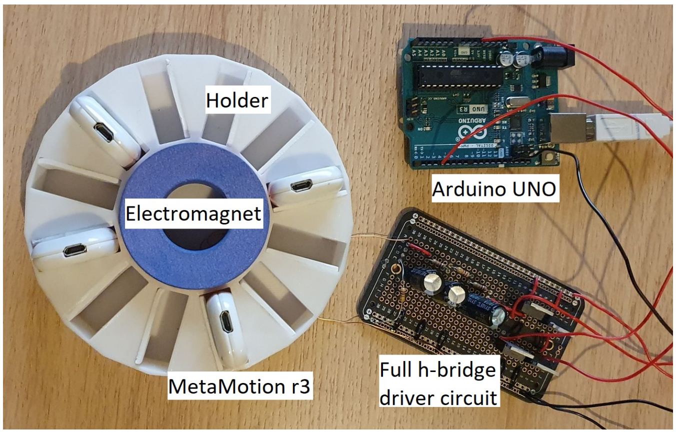

Figure 1. Experimental setup showing a simple 2W EMPG circuit and holder with 4 MetaMotion IMUs

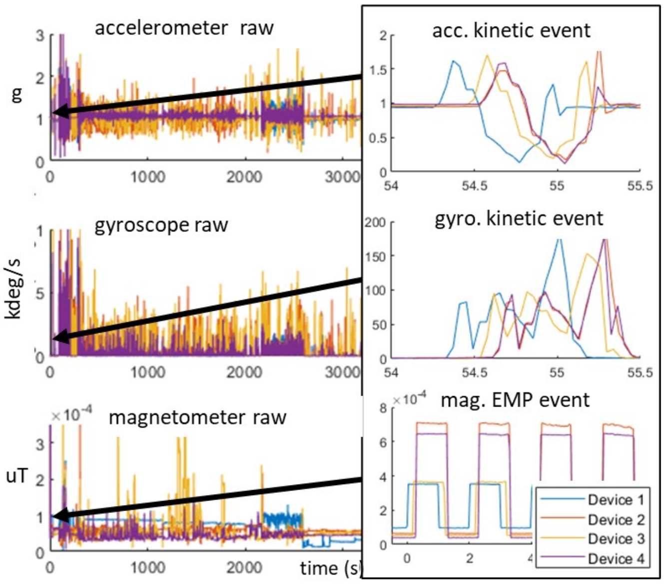

Figure 2. IMU magnitude data for 4 devices plotted against RTC time, highlighting "table slam" kinetic (accelerometer and gyroscope), and example of 4 equal-width EMP (magnetometer) pulses.

The rest of the paper is structured as follows: The preliminary proof-of-concept experiment and results are discussed (as originally presented in Gilbert et al. (2022)). We then introduce an extended method that improves synchronisation beyond the limitations of the sample frequency and describe an experimental setup to evaluate this. Finally we present the results of these experiments and discuss the wider practical implications of the work.

2 PRELIMINARY EMP STUDY

A simple electromagnetic pulse generator (EMPG) was built by attaching an electromagnet to an Arduino UNO via a full h-bridge, as shown in Figure 1. This EMPG was configured to transmit a 4 period length pulse at 0.5Hz. The electromagnet powered at 2W has a magnetic field strength of 0.2μT at 11cm. Below 0.2μT the magnetometer fails to measure the pulses giving an active range of 11cm.

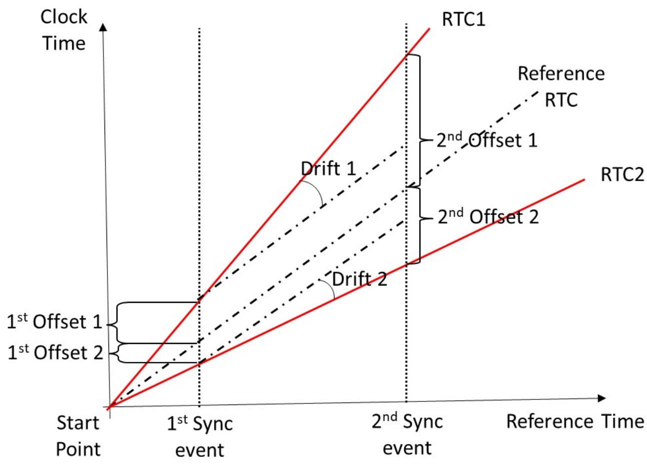

Figure 3. Timing diagram showing the offsets and drifts of 3 RTCs relative to one another.

Four MetaMotion R3 modules, from Mbientlabs Inc, USA, were set up using an iPad. Each module was configured to logging mode. The magnetometer is activated to record at 25Hz. Because the kinetic events will be used as an approximation of the 'gold standard' (having been used in many previous works) against which the magnetic method will be evaluated, the accelerometer and gyroscopes are sampled at a higher rate of 100Hz. The gyroscope was set to $\pm1600\ ^{\circ}/s$. The accelerometer was set to $\pm16gs$. The magnetometer's resolution is fixed at $\pm1300\mu T$. The only physical requirement of the magnetometer method is that the sensors are within range of the EMPG. However, to ensure the efficacy of the kinetic method, the modules are placed in a holder so that they might be moved in synchrony together, as shown in Figure 1.

Two synchronising events were generated at the start and end of the recording. A 4 period-length electromagnetic pulse (EMP) event was generated using the EMPG. A kinetic event as described in Ward et al. (2018) was then completed by swiftly lifting and slamming the holder on a table. The devices were then worn by the experimenter for approximately 1 hour of arbitrary movement. Afterwards the devices were returned to the holder and the EMP and kinetic event repeated.

The raw 3-axis accelerometer, gyroscope, and magnetometer data of the devices were uploaded to an iPad and saved for processing in MATLAB. The orientation-invariant magnitude (Euclidean norm) of each sensor was calculated and mapped relative to epoch time. The timestamps for each device's data are aligned at upload time to the iPad. This means that data points taken towards the end of the recording have the most accurate timing, with those towards the start of the recording subject to larger timing errors. The data for the 4 devices are plotted in Figure 2 with the first kinetic and EMP events magnified.

2.1 Preliminary Results

The data is aligned manually using the kinetic (accelerometer) events, this is done in a similar way to that described by Bannach et al. (2009). Specifically, the data is plotted and aligned manually until they appear most correlated according to the 'expert opinion' of the experimenter. To achieve this, an arbitrary device (device 1) is chosen as the reference to which all others are compared. The 1^{st} kinetic event for each device is then aligned by translating their data. With the 1^{st} events fixed, the data is then horizontally scaled (shortened or stretched) to align the 2^{nd} events.

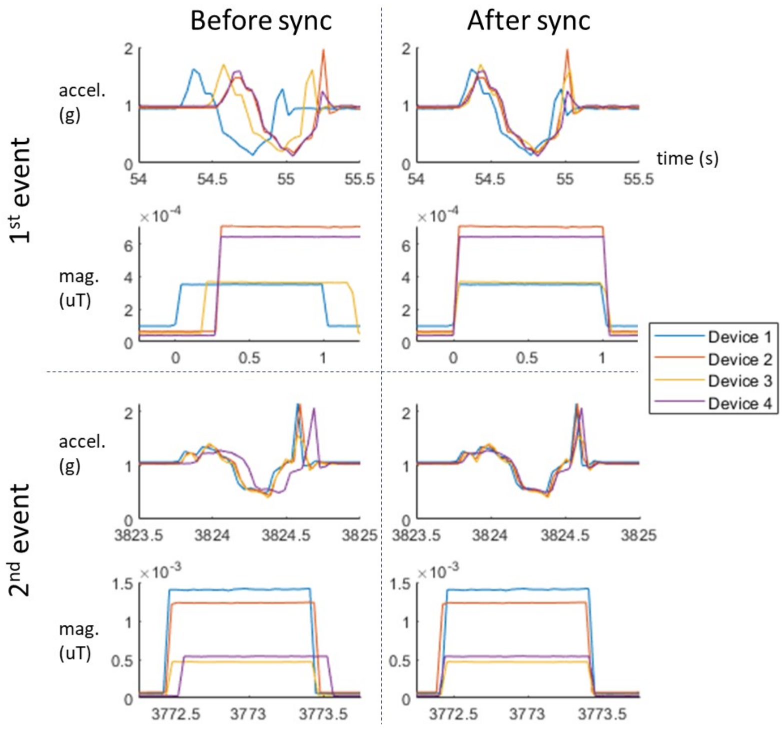

Figure 4. Closeups of 1^{st} and 2^{nd} kinetic (accel.) and EMP (mag.) events before and after synchronisation.

The RTC timing offsets for the two kinetic events (judged by expert opinion) are shown in Table 1. These show the offsets in ms of devices 2-4, relative to device 1. Note that after only 1 hour of recording, there is a large RTC offset of 267 ms between devices 1 and 2.

Table 1 also shows the relative clock drift, in parts-per-million (ppm), of each device's RTC. Drift is calculated using $10^6 * (D_d/D_1)$, where D_d is the difference in offsets between each event, and D_1 is the duration between the 1^{st} and 2^{nd} events for device 1. Refer to Figure 3 for a visual representation of the offsets and drift described in this paper.

The RTC crystal for each device has an accuracy of approximately ±40 ppm, so as the epoch time moves away from the RTC synchronisation point the offset error will increase. The drift shown in Table 1 between devices 1 and 2 of 67ppm indicates a large clock drift, but falling within the specified range ($< 40 + 40 = 80ppm$ for 2 devices).

To evaluate the EMP method, Devices 2-4 are re-aligned to device 1 by manually translating and scaling their data using the first rising edges of the 1^{st} and 2^{nd} EMP events. The difference between these EMP alignments and those of the kinetic events are shown in the rightmost columns of Table 1. A detailed plot of the events for the accelerometer and magnetometer before and after the EMP synchronisation process are shown in Figure 4.

2.1.1 EMP vs kinetic

Because there is no ideal ground truth for the timings, all results are calculated using distinguishable features in the data. One of the limitations on using kinetic events is that the signals have slight variations due to noise and micro-vibrations, thus making precise alignment challenging. This is one of the reasons that expert opinion is typically more accurate than automated correlational methods. Despite the fact that

		Timings based on RTC		Timings based on EMP event	
(Vs. device 1)	Drift (ppm)	1^{st} offset (ms)	2^{nd} offset (ms)	1^{st} offset (ms)	2^{nd} offset (ms)
Device 2	67.073	267	14	36	12
Device 3	39.502	168	19	34	10
Device 4	42.948	262	100	37	14

Table 1. Timing offsets between device 1 and the other IMU devices based on the RTC and EMP events for a 1 hour recording.

the devices in this experiment are fixed into a container and moved together, the variations in their kinetic responses can still be clearly seen in Figure 4.

In contrast, the rising and falling edges of the EMP events are relatively consistent across devices. The amplitude of the signals varies depending on the distance to the magnetic field generator, however this is less critical for synchronisation purposes. The defined edges remove the ambiguity associated with aligning a kinetic event. Because the shape and frequency of the EMP sequence are user-defined, it can be configured to provide additional information, such as unique identifiers to differentiate separate experiments or repeated sync events. In the rest of the paper, we make use of this flexibility to solve the problem of sample-rate limited accuracy.

2.1.2 Limitations on synchronisation accuracy

After EMP synchronisation, the offsets measured by the kinetic event for devices 2 to 4 are indistinguishable (<3ms). However, device 1 retains an offset of between 34 and 37ms compared to the other devices during the first event (as visible in the top right kinetic plot of Figure 4 and shown in the right 2 columns of Table 1). This post-synchronisation offset is a result of the limitation imposed by the sampling rate. With a sample period s, a lower than s alignment error cannot be guaranteed using only a single synchronisation edge. Given a sample frequency of 25Hz, a synchronisation error of up to $1/25$ =40ms is possible. In the case of the MetaMotion R3 the magnetometer can be configured to sample up to 300Hz giving a potential maximum error of approximately 3.3ms. However, such a high sample rate is not always possible - nor desirable - for some applications when battery life and storage capacity is an issue.

3 EXPANDED METHOD USING MULTIPLE PULSES

The accuracy of the fixed-pulse width method described above is fundamentally limited by the magnetometer sample rate. The expanded method described below bypasses this limitation by using a sequence of variable length pulses to locate a synchronisation event with sub-sample-rate accuracy. Specifically, the method involves transmitting a fixed-width pulse w followed by a sequence of slightly longer pulses until alignment is achieved.

The relationship between sample rate and capturing an EMP square wave can be formalised as follows. If we say that m is the difference between an EMP edge and the next sample point, then m must be $0 \leq m < s$ for a sample period of s. If the sample period decreases (rate increases), then the largest difference between the EMP edge and sample point will also decrease.

If a square pulse has a width of w and a sample period s, then it is expected that the pulse will be sampled $k = w/s$ times during its duration. Note that w should be a factor of s. However, if m is 0 an additional sample point is taken on the falling edge, making the total number of sample points $k + 1$, this phenomenon can be seen in Figure 5.

The expanded method uses this phenomenon to understand the alignment of the square EMP pulses to the set of captured samples. This is done by transmitting an initial square pulse with width w and several further pulses with a width of $w + a$, where a is the shift amount. This shift will result in the m value being reduced by the shift amount, a, after the next pulse, as shown after Pulse 1 in Figure 6. The following pulses will then have a distance $m - (p - 1)a$, where p is the pulse number, between the rising/falling edge and the first sample. With each successive pulse, the distance between an EMP edge and the first sample point will decrease. Eventually the distance will be small enough to allow an additional sample point. This can be seen for the 3 samples, highlighted by dashed red lines, that fit within Pulse 3 in Figure 6.

It is possible to determine within a range the initial m value from knowing the chosen a and which pulse has the additional sample point. For example if Pulse 1 has an additional sample point then $0 < m \leq a$, as this increase of a allows enough time for the additional sample point to occur on the pulse. Every subsequent pulse has an additional a shift from the initial pulse meaning $(p - 1)a < m \leq pa$ is true. Therefore the shift amount, a, can be seen as a parameter which sets the maximum error. However reducing a also increases the number of possible shifts required to guarantee an additional sample will capture a pulse. The minimum number of pulses required to guarantee the additional sample is $s/a + 1$. For example if the desired maximum error is 5ms and the sample period is 40ms, then the full synchronising signal will need to be at least 9 pulses long ($40/5 + 1 = 9$).

The transient response of the electromagnet is also a crucial limiting factor. The solenoid used in this experiment no longer had a stable transient response below a w of 300ms. Therefore considering that s must be a factor of w and the default s for the module used is 40ms, it was decided to use a w of 320ms. The length of the synchronising signal is then calculated by $s(w + a)/a + w$. With w =320ms, the 9 pulse sequence signal will take 2.92s.

3.1 Additional encoding

Although not essential for the functioning of the method described, it can be useful for some applications to encode further information into the EMP signal. For example, an identifying label might be added to address any issues with large offsets between the portable-EMPG RTC and any IMU RTC, which could lead to confusion and mis-identification of signals, see Figure 7.

Here we append a unique identifier number to the signal. This customisable label is appended after the synchronisation signal, facilitating correspondence between the central records on the EMP and the signals obtained from the IMUs. The trade-off, however, is an increase in signal length, resulting in an extended time required to transmit the sequence of pulses. The signal length is dependent on the w value as well as the desired identifier word length, n. The desired number of bits would be chosen considering the number of synchronisation events required for an experiment. In addition to the identifying bits, one start and one stop bit are added to the signal. The identifier length is approximately $w \times (n + 2)$. Therefore a 4-bit word identifier with a w value of 320ms would last an additional 1.92s.

If the de-synchronisation of EMP is negligible compared to the time between synchronising events, the removal of the identifier becomes a viable option, allowing for a reduction in synchronisation time without compromising the synchronisation quality.

3.2 Experimental setup

The EMPG of Figure 1 was adapted to incorporate an RTC such that the EMP events could have a centrally recorded reference timestamp. Additionally, the electromagnet was removed from the holder so

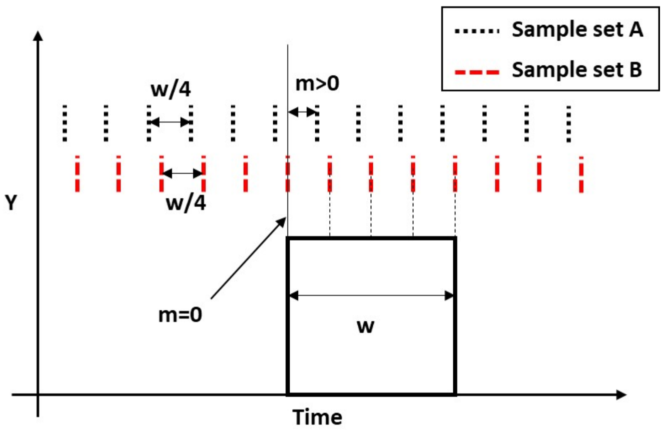

Figure 5. Example demonstrating how the alignment m dictates the number of samples capturing a pulse. Here the sample rate is $1/4$ pulse width, w. With $m > 0$ set A captures the pulse using 4 samples, while set B with $m = 0$ uses 5 samples.

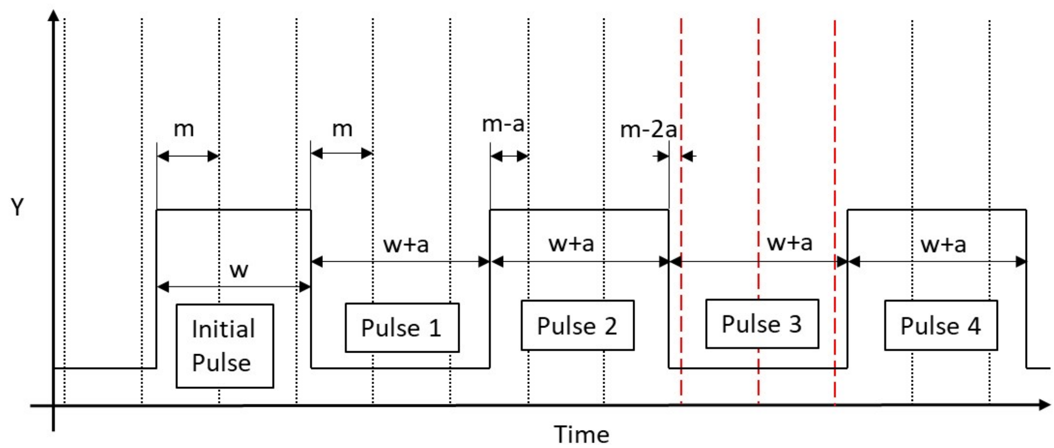

Figure 6. A graphical representation of the extended method demonstrating how the distance, **m**, between the starting edge of each pulse and the next sample reduces by the extended width, **a**. Note how pulses **1** and **2** only have two samples between the edges of the pulse, while pulse **3** has an additional sample point between its edges.

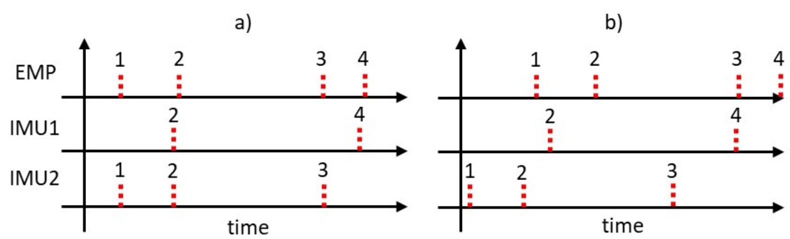

Figure 7. Example EMP events demonstrating typical and extreme de-synchronisation for two IMUs. a) Demonstrates how it is possible to associate the sync events from the portable-EMPG to the IMUs without a label using just their approximate location. b) Demonstrates how a greater offset between the RTCs of the portable-EMPG and the IMUs requires a label to determine which events belong together: for both IMU1 and IMU2 the 2^{nd} event could be mistaken for the 1^{st} if the labels were not present.

that it could be brought to individual IMUs. This new portable-EMPG uses a low-power electromagnet that could be directly powered by an Arduino MKR 1010 board (provided by SeeedStudios[1]). The experiment is conducted on a level surface, specifically a flat table, for two sessions of two hours each using multiple IMUs (MetaMotionRs) whose data is recorded through the MetaBase app. 8 IMU devices were set up to record accelerometer and magnetometer data at a sample rate of 25Hz. Meanwhile, a 60FPS video was recorded, showing a laptop displaying the Unix timestamp using the website (time.is/Unix_time) while the events occurred. This recording allowed a timestamp to be taken of the synchronisation events. This timestamp was then used to locate the events on MATLAB during post-processing.

The first event begins with generating an EM pulse using the portable-EMPG for each of the 8 IMUs. Following this, the IMUs are placed into a 3D-printed container, designed to reduce the independent motion of the devices. Once all are placed in the container, the container is quickly lifted and hit back onto the table, creating a kinetic event. Following two hours of recording arbitrary accelerometer and magnetometer data of the devices on the table, the IMU devices were removed from the container and the EMP event was repeated for each of the IMUs individually, while the IMUs were placed on the table with their Z axis facing up. Following this, the IMUs were placed back into the container and a second kinetic event was performed. The orientation-invariant magnitude (Euclidean norm) was calculated for all data.

3.3 Procedure

We conducted two separate 2-hour experiments to evaluate the method. One was conducted with an a value of 5ms, while the other involved a combination of 10ms and 20ms. These parameters were chosen based on successive halving of the sample period (40ms). The 2nd experiment, using 10 ms and 20 ms, demonstrates that rapid less accurate synchronisations as well as slower more accurate synchronisations can be performed within a single session. Each of the IMUs were synchronised using the methods previously described: using RTC timestamps only, using the original EMP method from the preliminary study, using the expanded EMP method described in this paper, and using cross-correlation of kinetic events. The cross-correlation of kinetic events was calculated by windowing the kinetic event, interpolating the timestamps and using the xcorr() method on MATLAB to determine the lag that results in the greatest correlation between the different IMUs; the IMUs time series were then translated by this lag value. All offsets are calculated with respect to the expert opinion based on the kinetic events.

3.4 Results

Figure 8 shows an example of the expanded EMP event sequence from one of the IMUs in this experiment. Note how the 3rd pulse has 9 sample points while the other pulses only have 8. This indicates that the EMP event is offset by up to 15ms (3*5ms) and must be adjusted accordingly.

The signal offsets for each IMU are presented in Table 2 (for a =5ms) and Table 3 (for a =10 and 20 ms) for the 4 synchronisation scenarios. The plots in Figure 9 also show the kinetic events of all IMUs across the four scenarios at a =5 ms.

As found in the preliminary study, the RTC-only synchronisation performs worse of all, with offset errors between 3 ms (Device 1) and up to 336 ms (Device 7). The original EMP method improves this by capping errors within the 40 ms sample period, with the largest error being 36 ms (Device 2).

Across all devices and a settings, the expanded method produces results most closely aligned with expert opinion. Table 2 reveals absolute offsets across the recording of no more than 7 ms for the expanded EMP

[1] SeeedStudios Grove Electromagnet: https://wiki.seeedstudio.com/Grove-Electromagnet/

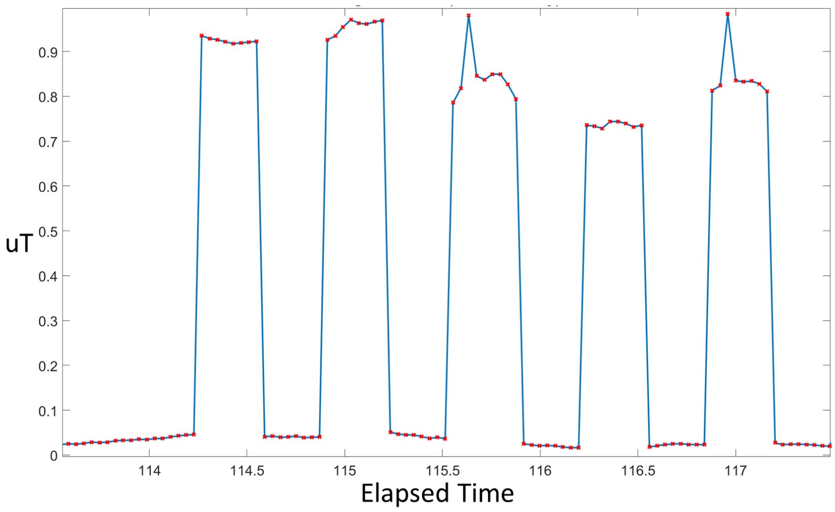

Figure 8. Electromagnetic pulses sampled by an IMU with the pulse width set to give a maximum error of $a = 5$ms. Note that the 9-sample situation occurs during the 3rd pulse.

	$a = 5$ ms							
IMU No.	1	2	3	4	5	6	7	8
RTC sync	3	64	-95	-150	108	-56	-336	30
Original EMP	3	-36	15	12	-14	-21	-4	-23
Expanded EMP	6	-4	3	-7	-1	-5	-4	0
KE+CC	3	23	-24	-23	28	-15	-13	30

Table 2. Offsets (in ms) vs expert opinion for 4 mehods: RTC synchronisation, original EMP method, expanded EMP method with a =5 ms, and kinetic event + cross-correlation method.

method (Device 4), as comparable to offsets of up to 36 ms for the original EMP (Device 2). Similarly, for the 2nd experiment with $a = 10$ in Table 3, the maximum recorded offset is 10 ms (Device 3), and for $a = 20$, the maximum is 18 ms (Device 7). These values align closely with what might be expected from the desired a settings.

Although most of the results for the expanded method fall within the specified a value, for 2 devices the offset rises above this (Devices 1 and 4 in Table 2). This is explained by the additional transient response time of the electromagnet, which can be up to 3 ms. So whereas in an ideal system the offset error would be capped at a, in a real system this would actually be $(a + 3)$ ms.

Notably, the kinetic cross-correlation method achieves a very high variability in error - from between 3 ms (Device 1, Table 2) to as much as 142 ms (Device 7, Table 3). This can best be explained by the reliance of this method on calculating correlations across accelerometer signals that are noisy. Although plot (c) in Figure 9 achieved the highest between device correlation scores, it is clearly not as well aligned as the expert-based alignment of plot (e) - or indeed the expanded EMP method shown in plot (d).

4 DISCUSSION

The main goal of this paper is to demonstrate an in-situ synchronisation method which is able to achieve sub sample accuracy without requiring any modifications to the hardware or firmware of commercial IMUs.

	a =10 ms				a =20 ms			
IMU No.	1	2	3	4	5	6	7	8
RTC sync	-26	114	-68	-143	117	-22	-322	6
Original EMP	16	-26	3	-8	-11	26	0	-9
Expanded EMP	6	0	10	0	-10	10	18	-5
KE+CC	-26	7	-67	-58	117	102	142	87

Table 3. Offsets (in ms) vs expert opinion for 4 mehods: RTC synchronisation, original EMP method, expanded EMP method wth a =10 ms (IMU1-4) and a =20 ms (IMU5-8), kinetic event + cross-correlation.

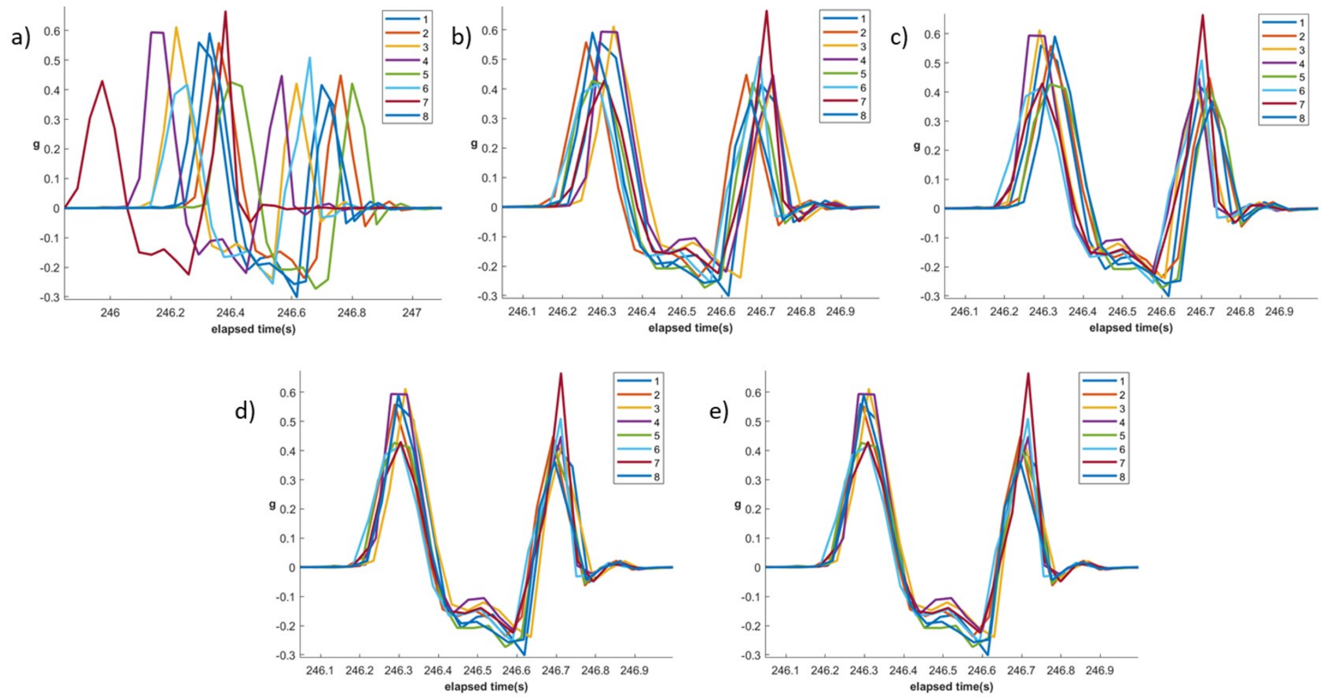

Figure 9. The 1^{st} kinetic event signals of 9 devices after a) RTC sync b) standard EMP sync c) kinetic event + cross corr d) expanded EMP sync e) expert opinion. Note that the output obtained using the expanded method is most similar to the expert opinion.

A simple method of using electromagnetic pulses was first demonstrated that achieves an accuracy dependent on the sample frequency. An expanded method then demonstrated how sub-sample accuracy can be achieved using encoded pulses and a central RTC.

Unlike in similar methods, the method demonstrated here does not heavily rely on the amplitude of the recorded event. The method only requires that the edges of the synchronising signal are distinguishable. The distances between the IMU devices and the synchronising unit do not need to be fixed, instead the IMU device must only be within the active range of the portable-EMPG. This means IMU devices are not required to be removed from their experimental setup to be synchronised, which is particularly useful when deploying a large number of IMU devices in wearables. Similar methods require the devices to be removed from the participants and placed into a synchronisation box, which when working with a large number of IMUs can be a long process prone to mislabelling. Additionally, the size of the synchronisation box limits the number of IMUs that can be used in the experiment as similar methods require all the devices to be synchronised simultaneously. The method demonstrated by this paper does not require a synchronisation box nor simultaneous synchronisation meaning there is no limit to the number of IMUs that be synchronised.

Two configurations of the expanded multi-pulse method were demonstrated, with the maximum error parameters set as $a = 5$ms and a combination of $a = 10$ms and $a = 20$ms. Note all three accuracy values are sub-sample accuracy, which for a 25Hz magnetometer is 40ms. The first configuration shows how the method can be used to achieve low synchronisation offset comparable to similar studies, while the second configuration shows how the user could choose to go with quicker synchronisation events when low offsets are not required. Additionally, the second configuration also shows how multiple offset values can be used in a single session, giving the user of the method even more flexibility, allowing them to choose an appropriate offset on the fly in response to live events.

4.1 Limitations

Although the expanded method synchronises IMUs using the edges rather than the amplitude of the received signals, it still needs to be guaranteed that the signal can be distinguished from the noise background. Currently, the system is limited by the Electromagnetic Field (EMF) Regulations from applying powerful electromagnets ICNIRP (2009). This constrains the maximum effective distance for synchronisation between EMPG and IMUs. The current active range of 11cm limits the number of applications this method will be effective in, requiring small synchronisation points. One caveat to this limitation is that the portability of the proposed method, and the fact that a central reference RTC is used, means that these synchronisation points can simply be brought close to wherever each IMU is located if the experiment permits it.

A further limitation of this method is that the synchronisation of all devices is dependent on the central RTC of the EMPG. This RTC is also susceptible to drift. Figure 3 is a timing diagram showing the offsets and drifts associated with the inaccuracies of an RTC. This diagram shows how two IMUs with opposing offsets and drifts can result in large de-synchronisation of clocks. Note that in this diagram the drift of the electromagnetic generator's RTC is less than the two IMUs, in practice this may not be the case as this method is focused on synchronising the clocks of multiple IMUs rather than determining absolute timing.

In situations where the portable-EMPG's RTC could induce significant desynchronisation, then an additional 6-bit identifier can be appended to the signal to help differentiate sync events. The downside to this is that it would result in an extended synchronisation time (1.92s in the example given in this paper).

Overall, the expanded method can achieve higher synchronisation performance by increasing the signal length; however, degree of accuracy is constrained by the transient response of the electromagnet. In experiments, the transient response resulted in an approximate width of 3 ms for each edge, which is a factor that should be taken into consideration when employing this approach.

5 CONCLUSION

This paper introduces a new method for synchronizing wearable IMUs using a portable electromagnetic pulse generator (portable-EMPG) to transmit magnetic pulses. This approach potentially enables synchronisation of multiple wearable IMUs without requiring their removal from users. Through experiments with different maximum degrees of error (5ms, 10ms, and 20ms), we demonstrate the method's flexibility in adjusting synchronisation accuracy to user requirements. The trade-off is that more precise synchronisation requires a longer sequence of EMP events. Additionally, we introduce the idea of using further encoding on the electromagnetic pulse to act as an identifier, allowing the user to identify specific events with a binary word.

Our study identifies a 3ms error related to the solenoid's transient response and acknowledges drift and offset errors associated with synchronizing to a central RTC. Future research will focus on extending the portable-EMPG's active range and improving timestamp accuracy through Wi-Fi integration. These advancements aim to enhance the reliability and effectiveness of the synchronisation technique, making it applicable across various domains reliant on precise IMU data synchronisation. This work contributes to the development of synchronisation methodologies in inertial measurement systems, promising improved data accuracy and usability in practical applications.

AUTHOR CONTRIBUTIONS

TG and ZL are joint first authors of this work. TG conducted the initial study, and ZL developed and evaluated the follow-on work. TG, ZL, and JW contributed equally to the development of the concept, interpretation of the results and presentation of the manuscript. SD and AH provided additional intellectual contributions towards the concept and final manuscript.

FUNDING

This work is funded in-part by the ERC SocSensors project (Ref: 899779).

DATA AVAILABILITY STATEMENT

The datasets and and Matlab code for this study are available here: github.com/jThumus/Electromagnetic-synchronisation-of-multiple-IMUs.

REFERENCES

Bannach, D., Amft, O., and Lukowicz, P. (2009). enAutomatic Event-Based Synchronization of Multimodal Data Streams from Wearable and Ambient Sensors. In *Smart Sensing and Context*, eds. P. Barnaghi, K. Moessner, M. Presser, and S. Meissner (Berlin, Heidelberg: Springer), Lecture Notes in Computer Science, 135–148. doi:10.1007/978-3-642-04471-7_11

Bian, S., Liu, M., Zhou, B., and Lukowicz, P. (2022). The state-of-the-art sensing techniques in human activity recognition: A survey. *Sensors* 22, 4596

Bulling, A., Blanke, U., and Schiele, B. (2014). A tutorial on human activity recognition using body-worn inertial sensors. *ACM Computing Surveys (CSUR)* 46, 1–33. Publisher: ACM New York, NY, USA

Gao, N., Shao, W., Rahaman, M. S., and Salim, F. D. (2020). n-gage: Predicting in-class emotional, behavioural and cognitive engagement in the wild. *Proc. ACM Interact. Mob. Wearable Ubiquitous Technol.* 4. doi:10.1145/3411813

Gilbert, T., Day, S., Hamilton, A. F. D. C., and Ward, J. (2022). A simple method for synchronising multiple imus using the magnetometer. In *Proceedings of the 2022 ACM International Symposium on Wearable Computers* (New York, NY, USA: Association for Computing Machinery), ISWC '22, 100–102. doi:10.1145/3544794.3558466

Gravina, R., Alinia, P., Ghasemzadeh, H., and Fortino, G. (2017). Multi-sensor fusion in body sensor networks: State-of-the-art and research challenges. *Information Fusion* 35, 68–80

Guo, X., Mohammad, M., Saha, S., Chan, M. C., Gilbert, S., and Leong, D. (2016). PSync: Visible light-based time synchronization for Internet of Things (IoT). In *IEEE INFOCOM 2016 - The 35th Annual IEEE International Conference on Computer Communications*. 1–9. doi:10.1109/INFOCOM.2016.7524358

Hoelzemann, A., Odoemelem, H., and Van Laerhoven, K. (2019). Using an in-ear wearable to annotate activity data across multiple inertial sensors. In *Proceedings of the 1st International Workshop on Earable Computing*. 14–19

ICNIRP (2009). Icnirp statement on the "guidelines for limiting exposure to time-varying electric, magnetic, and electromagnetic fields (up to 300 ghz)". *Health physics* 97, 257–258

Idrees, Z., Granados, J., Sun, Y., Latif, S., Gong, L., Zou, Z., et al. (2020). IEEE 1588 for clock synchronization in industrial IoT and related applications: a review on contributing technologies, protocols and enhancement methodologies. *IEEE Access* 8, 155660–155678. Publisher: IEEE

Li, D. and Sinha, P. (2012). Rbtp: Low-power mobile discovery protocol through recursive binary time partitioning. *IEEE Transactions on Mobile Computing* 13, 263–273. Publisher: IEEE

Luo, C., Koski, H., Korhonen, M., Goncalves, J., Anagnostopoulos, T., Konomi, S., et al. (2017). Rapid clock synchronisation for ubiquitous sensing services involving multiple smartphones. In *Proceedings of the 2017 ACM International Joint Conference on Pervasive and Ubiquitous Computing and Proceedings of the 2017 ACM International Symposium on Wearable Computers* (New York, NY, USA: Association for Computing Machinery), UbiComp '17, 476–481. doi:10.1145/3123024.3124432

Plotz, T., Chen, C., Hammerla, N. Y., and Abowd, G. D. (2012). Automatic Synchronization of Wearable Sensors and Video-Cameras for Ground Truth Annotation – A Practical Approach. In *2012 16th International Symposium on Wearable Computers*. 100–103. doi:10.1109/ISWC.2012.15. ISSN: 2376-8541

Raman, C., Tan, S., and Hung, H. (2020). A modular approach for synchronized wireless multimodal multisensor data acquisition in highly dynamic social settings. In *Proceedings of the 28th ACM International Conference on Multimedia* (New York, NY, USA: Association for Computing Machinery), MM '20, 3586–3594. doi:10.1145/3394171.3413697

Rowe, A., Gupta, V., and Rajkumar, R. (2009). Low-power clock synchronization using electromagnetic energy radiating from ac power lines. In *Proceedings of the 7th ACM Conference on Embedded Networked Sensor Systems*. 211–224

Spilz, A. and Munz, M. (2023). Synchronisation of wearable inertial measurement units based on magnetometer data. *Biomedical Engineering/Biomedizinische Technik*

Sun, Y., Greaves, D. A., Orgs, G., de C. Hamilton, A. F., Day, S., and Ward, J. A. (2023). Using wearable sensors to measure interpersonal synchrony in actors and audience members during a live theatre performance. *Proceedings of the ACM on Interactive, Mobile, Wearable and Ubiquitous Technologies* 7, 1–29

Wang, C., Sarsenbayeva, Z., Luo, C., Goncalves, J., and Kostakos, V. (2019). Improving wearable sensor data quality using context markers. In *Adjunct Proceedings of the 2019 ACM International Joint Conference on Pervasive and Ubiquitous Computing and Proceedings of the 2019 ACM International Symposium on Wearable Computers*. 598–601

Ward, J. A., Pirkl, G., Hevesi, P., and Lukowicz, P. (2017). Detecting physical collaborations in a group task using body-worn microphones and accelerometers. In *2017 IEEE International Conference on Pervasive Computing and Communications Workshops (PerCom Workshops)*. 268–273. doi:10.1109/PERCOMW.2017.7917570

Ward, J. A., Richardson, D., Orgs, G., Hunter, K., and Hamilton, A. (2018). Sensing Interpersonal Synchrony between Actors and Autistic Children in Theatre Using Wrist-Worn Accelerometers. In *Proceedings of the 2018 ACM International Symposium on Wearable Computers* (New York, NY, USA: Association for Computing Machinery), ISWC '18, 148–155. doi:10.1145/3267242.3267263. Event-place: Singapore, Singapore

Wolling, F., Huynh, C. D., and Van Laerhoven, K. (2021a). Ibsync: Intra-body synchronization of wearable devices using artificial ecg landmarks. In *Proceedings of the 2021 ACM International Symposium on Wearable Computers*. 102–107

Wolling, F., van Laerhoven, K., Siirtola, P., and Röning, J. (2021b). Pulsync: The heart rate variability as a unique fingerprint for the alignment of sensor data across multiple wearable devices. In *2021 IEEE International Conference on Pervasive Computing and Communications Workshops and other Affiliated Events (PerCom Workshops)*. 188–193. doi:10.1109/PerComWorkshops51409.2021.9431015

Yan, Z., Tan, R., Li, Y., and Huang, J. (2019). Wearables Clock Synchronization Using Skin Electric Potentials. *IEEE Transactions on Mobile Computing* 18, 2984–2998. doi:10.1109/TMC.2018.2884897. Conference Name: IEEE Transactions on Mobile Computing